L-Phenylalanine Partitioning Mechanisms in Model Biological Membranes

Katelyn M. Duncan[†,a], Rhys C. Trousdale[†,a], Cristina Gonzales[‖], William H. Steel[‡], and Robert A. Walker[†§]*

.

[†]Department of Chemistry and Biochemistry, Montana State University, Bozeman, Montana 59717, United States.

[‖]Department of Chemistry, Reed College, Portland, Oregon 97202, United States

[‡]Department of Chemistry, York College of Pennsylvania, York, Pennsylvania 17403, United States

[§]Montana Materials Science Program, Montana State University, Bozeman, Montana 59717, United States

[a]Both authors contributed equally to this work.

KEYWORDS: L-Phenylalanine, membrane partitioning, lipid membranes, time-resolved fluorescence, TCSPC, DSC

Abstract.

Time-resolved fluorescence spectroscopy in combination with differential scanning calorimetry (DSC) was used to study the chemical interactions that occur when L-Phenylalanine is introduced to solutions containing phosphatidylcholine vesicles. Studies reported in this work address open questions about L-Phe's affinity for lipid vesicle bilayers, the effects of L-Phe partitioning on bilayer properties, L-Phe's solvation within a lipid bilayer, and the amount of L-Phe within that local solvation environment. DSC data show that L-Phe reduces the amount of heat necessary to melt saturated phosphatidylcholine bilayers from their gel to liquid-crystalline state but does not change the transition temperature ($T_{gel\text{-}lc}$). Time-resolved emission shows only a single L-Phe lifetime at low temperatures corresponding to L-Phe remaining solvated in aqueous solution. At temperatures close to $T_{gel\text{-}lc}$, a second, shorter lifetime appears that is assigned to L-Phe already embedded within the membrane that becomes hydrated as water starts to permeate the lipid bilayer. This new lifetime is attributed to a conformationally restricted rotamer in the bilayer's polar headgroup region and accounts for up to 30% of the emission amplitude. Results reported for dipalmitoylphosphatidylcholine (DPPC, 16:0) lipid vesicles prove to be general with similar effects observed for dimyristoylphosphatidylcholine (DMPC, 14:0) and distearoylphosphatidylcholine (DSPC, 18:0) vesicles. Taken together, these results create a complete and compelling picture of how L-Phe associates with model biological membranes. Furthermore, this approach to examining amino acid partitioning into membranes and the resulting solvation forces points to new strategies for studying the structure and chemistry of membrane soluble peptides and selected membrane proteins.

Introduction. Small molecule accumulation in lipid membranes can have far reaching effects on membrane properties. Solutes such as chloroform, diethyl ether, and others have long been known to have anesthetic effects.[1, 2] Fat soluble vitamins such as vitamins A and E serve as antioxidants, protecting lipid membranes from reactive oxygen species.[3] Small molecule partitioning into lipid membranes can also result in cell death through deactivating transmembrane ion channels and subsequent accumulation of reactive oxide species.[4-6] Historically, a solute's tendency to partition is empirically predicted by the partitioning coefficient (logP) that calculates a solute's solubility preference for an organic (1-octanol) phase in comparison to an aqueous phase.[7] LogP has long historical relevance and is still being used today in agriculture and pharmaceuticals.[8, 9] While logP is a useful, zeroth-order predictor, it is still a solubility argument and therefore does not account for the chemical complexity found within biological membranes. Understanding specific chemical interactions that occur is important as actual partitioning behavior depends on much more than calculated and measured molecular properties used to develop quantitative structural activity relationships (QSARs) and linear solvation free energy relationships (LSERs).[10-13]

To identify and isolate solute-membrane interactions, biological membranes are often simplified and represented by pure lipid bilayer vesicles. Real biological membranes are decidedly complex in nature as they include proteins, carbohydrates, and cholesterol within the bilayer as depicted in the fluid mosaic model.[14, 15] In this context amino acids play an important role as changing individual residues on membrane peptides and proteins can change structure, orientation and stability.[16-18] Amino acids in membrane proteins have also been used as sensors of a membrane's physical state.[19, 20]

Specific to Phenylalanine (Phe or L-Phe), L-Phe aggregate interactions with membranes is responsible for the inherited disease, phenyketonuria (PKU). Model membranes were used to study how phenylalanine interacts with biological membranes.[21, 22] One study analyzed oleic acid vesicles and a fluorescent probe to analyze Phe's effects on vesicle properties and found Phe reduces vesicle rigidity and changes membrane hydration.[23] Another study analyzed L-Phe's effects on lipid monolayers and discovered L-Phe integrates into the film and affects surface tension, phase morphology and ordering of the lipid film.[24] While instructive, neither of these studies were able to quantify the amount of L-Phe that could be accommodated by a lipid membrane, nor *where* within the membrane L-Phe or its aggregates were accumulating.

A recent study by Perkins *et. al.* found that Phenylalanine (L-Phe, Phe) increases membrane permeability.[21] Using cryo-TEM, the authors proposed that Phe aggregated to form fibrils that reduced membrane rigidity making it more permeable. Motivated by this study, recent work in our lab studied the effects that the isomer L-Phe has on coumarin partitioning in lipid bilayer vesicles.[25] Results showed that L-Phe increased *relative* solute partitioning into the lipid bilayer's nonpolar region but blocked a large amount of solute from partitioning while the lipid was in the rigid and structured gel phase.[25]

The calculated logP value for L-Phe is -1.4 in the uncharged, neutral phase indicating a solubility preference for the aqueous environment rather than the organic phase.[7, 25, 26] However, at a biologically relevant pH (~7.4), L-Phe is zwitterionic, and although the net charge is zero, its logP value rises to 0.12 predicting that L-Phe is just as likely to partition into a polar organic phase as remain in an aqueous phase. Initial literature reports by Chakrabarti et al. predicted that only the uncharged neutral – not zwitterionic – form of L-Phe permeates into the membrane and comprises only a small fraction of the total amount of L-Phe in solution.[27, 28] However, more recent studies

determined L-Phe in its zwitterionic form permeates deeper into the membrane allowing L-Phe monomers to be more dynamic as they interact with the lipid.[24] The zwitterionic L-Phe intercalates into the polar headgroup of the lipid, primarily through membrane deformities when the membrane is in its frozen gel phase.[24, 26-29] Computational studies show that L-Phe's aromatic ring increases the solute's tendency to enter into the lipid bilayer displacing the water that is in the polar headgroup creating a polar aprotic environment.[26] L-Phe then arranges itself with its aromatic ring aligning normal to the nonpolar acyl chains.[30-33]

L-Phe is one of three aromatic amino acids that are naturally fluorescent and contribute to protein fluorescence. L-Phe is the least fluorescent of the three of aromatic amino acids with a quantum yield of 0.023 in an aqueous solution. For comparison, the quantum yields for Tyrosine (Tyr) and Tryptophan (Trp) are 0.14 and 0.13, respectively.[34-37] Interestingly, L-Phe does not directly contribute to a protein's fluorescence emission as it efficiently transfers its energy to Tyr then to Trp. Because of this lack of direct contribution to protein fluorescence and low quantum yields, the excited state photochemistry of L-Phe has not been studied as thoroughly as for Tyr and Trp.[34, 38-42] The emission behavior of L-Phe has been studied with differing functional groups in effort to understand how each addition affects its photphysical properties.[43, 44] Phenylalanine's behavior in a short peptide was characterized when phenylalanine and serine were analyzed as monomers in the gas phase and then again in its excited state as the two monomers dimerized and relaxed to form a short chain dipeptide.[40]

In most of the studies described above, L-Phe and other amino acids have been analyzed indirectly either by using a fluorescent probe or through computational studies intended to predict L-Phe partitioning into membranes.[45] These surrogate studies were simpler to carry out relative to direct measurements due to L-Phe's intrinsically low fluorescence yields. Findings reported below

measure L-Phe's partitioning behavior *directly* using time-resolved fluorescence spectroscopy in four different lipid bilayer systems. Using time-resolved and steady-state fluorescence spectroscopy, this work examines the chemical interactions that occur when L-Phe is introduced to a model biological membrane. Specifically, these studies identify *where* within the membrane does L-Phe integrate; *how much* L-Phe partitions within the heterogeneous membrane environment; and the effects L-Phe has on the lipid bilayer properties.

Experimental Methods.

Materials

L-Phenylalanine (L-Phe) was purchased from Alfa Aesar and used as received. Organic solvents used were purchased from Sigma-Aldrich and used as received. Millipore water (18.2 MΩ) was used to make the vesicle solutions. The vesicle solutions consisted of an aqueous solution containing 0.84 g of sodium bicarbonate (Sigma Aldrich, 99.99%) with the pH adjusted to 7.0 ± 0.1 at 20˚C using concentrated HCl. Allowing for the Na^+ and HCO_3^- concentrations at pH 7, vesicle solution ionic strength 47.5 mM. 1,2-dilauroyl-*sn*-glycero-3-phosphocholine (12:0 DLPC), 1,2-dimyristoyl-*sn*-glycero-3-phosphocholine (14:0 DMPC), 1,2-Dipalmitoyl-*sn*-glycero-3-phsophocholine (16:0 DPPC), and 1,2-distearoyl-*sn*-glycero-3-phosphocholine (18:0 DSPC) were purchased from Avanti Polar Lipids (Alabaster, AL) and used as received. Vesicle solutions were prepared with 1.5 mM lipid content for fluorescence experiments and 20 mM lipid content for DSC measurements. Structures of all molecules can be found in Supporting Information (bSI-1).

Lipid Bilayer Vesicle Preparation

Lipid bilayer vesicles were prepared by dissolving the lipid in chloroform and subsequently drying the solution via rotary evaporation. The resulting thin lipid film was then rehydrated using a 10 mM L-Phe in the pH 7 carbonate solution to form a solution with multilamellae lipid bilayers.

While the carbonate concentration of this solution is not sufficiently high to be considered a buffer, we noted that adding the L-Phe to the solution changed the overall solution pH by less than 0.02.

Our choice of 10 mM L-Phe for these experiments was the result of two conflicting considerations. The low quantum yield of L-Phe encouraged experiments to be performed at higher concentrations for better S/N. However, we also wished to work with low L-Phe concentrations to minimize the possibility of aggregation effects. To ensure that the 10 mM results were the result of L-Phe monomers either in bulk aqueous solution or partitioned into the bilayer, we performed a series of fluorescence emission measurements using 2.5 mM L-Phe. These results are shown in Supporting Information (Figures SI-2 and SI-3 and Table SI-1). Close agreement in the data from these two systems implies that L-Phe aggregation is not an important consideration at 10 mM.

Solutions were sonicated for 30 minutes at temperatures 10 °C higher than each lipid's respective gel-liquid crystalline transition temperature ($T_{gel\text{-}lc}$). The solution then extruded through a PTFE syringe filter (450 nm) to remove giant unilamellar vesicles. Solutions were again heated to 10 °C higher than $T_{gel\text{-}lc}$ and extruded through an Avanti Mini Extruder 11 times with a membrane pore size of 200 nm. Vesicles sizes were determined via Dynamic Light Scattering analyses (Figures SI-4 and SI-5, and Table SI-2), showing that the Pure DPPC and DPPC with L-Phe had diameters of 132 and 166 nm respectively.

Differential Scanning Calorimetry (DSC)

Differential scanning calorimetry (DSC) measurements were performed using a TA instruments Discovery DSC 2500. The vesicles for DSC experiments were not filtered to any specific vesicle size. For experiments, Tzero pans and Tzero hermetic lids (TA instruments) were used. To prepare the sample 2 ± 0.1 mg of a vesicle solution was added to the pans and the samples were sealed. Care was taken to ensure that the entire solution was deposited *in* the pan and no stray

drops touched the pan. Except for experiments with DLPC, temperature scans began at 15 °C below the $T_{gel\text{-}lc}$ and heated 1°C/min to 15 °C above the $T_{gel\text{-}lc}$ to capture the full gel-liquid crystalline transition temperature ($T_{gel\text{-}lc}$). (DSC experiments with DLPC began at temperatures near -5˚C, only 3˚ below DLPC's $T_{gel\text{-}LC}$ of -2˚C.)

Time-Correlated Single-Photon Counting (TCSPC)

Fluorescence experiments were measured following L-Phenylalanine excitation by a Ti:sapphaire oscillator (Coherent Chameleon, 80 MHz, 85 fs pulse duration, 680-1040 nm wavelength range) coupled with an APE autotracker harmonic generator used to frequency triple the fundamental wavelength. A Conoptics model 350-80 modulator was used to reduce the repetition rate to 4 MHz. Picoquant PicoHarp 300 and FluoTime 200 software were used for data collection. Samples were equilibrated at the reported temperatures for 5 minutes using a Quantum Northwest TC125 control (Seattle, WA). A long pass filter (90% transmission >280 nm) was placed after the sample to reduce scattering from the vesicles. Photon emission was collected at 290 nm, a wavelength that overlapped all emission spectra in bulk solvents. Excitation wavelength chosen was 260 nm for all solutes, a wavelength that overlapped in each of the bulk solvents.

Time-resolved emission data from vesicle-containing solutions were fit with a linear combination of independent lifetimes and amplitudes using fitting parameters that are adjusted to minimize residuals and optimize χ^2. The resulting fluorescent lifetimes were then compared to the lifetimes of the solute in different solvents chosen to mimic local solvation environments within the lipid bilayer. The fluorescence decay and amplitude expression are shown in Eq. 1, where A_i and τ_i are the amplitude and the lifetime of the i^{th} component, respectively.

$$I(t) = \int_0^t IRF\,(t') \sum_{i=1}^{n} A_i e^{-\frac{t-t'}{\tau_i}}\, dt' \qquad (1)$$

Each trace was fit independently, without any constraints, for the lifetimes and amplitudes. The typical χ^2 were from 0.9-1.1 when accounting for at most three lifetimes. Typically, uncertainties in lifetimes and amplitudes were 0.2 ns and 0.04, respectively. There is an inherent uncertainty in the lifetimes reported of ± 0.3 ns due to the detection limit of the instrument; however, the data and error bars presented in this work represent results from at least 3 independently prepared, equivalent trials averaged together with a single population standard deviation of those trials. The average lifetime and amplitudes and their respective standard deviations are reported for each specific temperature and only compared to their respective temperature.

Results.

Analyzing L-Phe's effect on DPPC lipid vesicles with DSC

To understand how, or even if, L-Phe interacts with DPPC bilayers, differential scanning calorimetry (DSC) was employed to understand the effect L-Phe has on bilayer properties. Two separate lipid vesicles solutions at a 20 mM concentration were hydrated with a carbonate-containing aqueous solution with and without L-Phe. Previous work has shown that small solutes associating with lipid bilayers can disrupt monomer-monomer interactions leading to a decrease in the bilayer gel to the liquid-crystalline phase transition temperature ($T_{gel\text{-}lc}$). [46, 47] Alternatively, some studies have reported that strong solute-headgroup association can dehydrate the membrane's outer layer, enhancing monomer-monomer interactions and *increasing* $T_{gel\text{-}lc}$.[48, 49]

The DSC traces of DPPC lipid vesicles with and without L-Phe show that the $T_{gel\text{-}lc}$ remained unchanged from the addition of the amino acid to the vesicle system (Figure 1). However, the addition of L-Phe to the lipid bilayer vesicle resulted in a decrease in the heat flow required to

drive the gel phase into the liquid-crystalline phase transition with a slight, asymmetric widening of the peak base to lower temperatures.

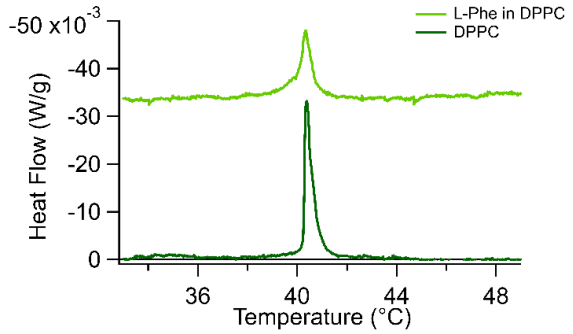

Figure 1. DSC spectra of pure DPPC vesicle solutions and DPPC vesicle solutions containing 10 mM L-Phe. The two endotherms are offset for the ease of viewing.

From this result, we infer that any L-Phe that does partition into the bilayer has minimal effect on the cohesive chain-chain interactions, although any impact is assumed to be weakly disruptive given the subtle low-temperature tailing in the DSC trace. Such a result could arise if L-Phe in the bilayer disrupted local acyl chain interactions without disrupting the overall long-range order characteristic of DPPC bilayers in their gel state. This suppression of heat flow is monotonic with L-Phe concentration. We performed equivalent experiments with solutions containing less L-Phe (1, 6, and 8 mM) and noted that while the endotherm grew in magnitude, even at 1 mM, the maximum heat flow was still 25% smaller than the pure DPPC endotherm. These data are shown in Supporting Information (Figure SI-6.)

DLS measurements of DPPC vesicles in aqueous solution both with and without L-Phe support this interpretation. Adding L-Phe to DPPC-containing solutions leads to a ~25% increase in the vesicle diameter and significantly broadens the distribution, again implying some disruption in the lipid bilayer, but not enough to changes the fundamental thermodynamics of the gel-liquid crystalline transition. (DLS results for DPPC vesicles in aqueous solution and solutions containing 5 and 10 mM L-Phe are shown in Supporting Information, (Figures SI-5 and Table SI-2).

TCSPC of L-Phe in model bulk solvents.

To evaluate the partitioning mechanisms of L-Phe, we first analyzed L-Phe's fluorescence behavior in bulk solvents chosen to model the possible local solvation environments of a lipid bilayer vesicle: acetonitrile for a polar aprotic environment, methanol for a polar, protic environment, and cyclohexane to model the hydrophobic region created by the hydrocarbon tails. This approach has been used previously to identify changes in solvation opportunities within the membrane interior as the membrane melts.[25, 50-52] One important consideration is that the region created by the lipid glycero-backbones is polar and intrinsically aprotic. Only when water begins hydrating this region is there any opportunity for hydrogen bond formation. Water is expected to percolate into the membrane as the membrane adopts its 'ripple phase' or, equivalently, in the vicinity of its gel-liquid crystalline pre-transition.[53] DPPC's ripple phase occurs at 35 °C.[54, 55]

The lipid bilayer vesicles used in this study are prepared in a 10 mM a pH 7 aqueous solution. Consequently, similarities in L-Phe emission lifetimes in the aqueous solution and in solutions containing DPPC vesicles are attributed to L-Phe solutes that do not associate with the bilayer. L-Phe lifetimes in DPPC lipid vesicle solutions are determined independently from the daa without consideration of what was measured in the different bulk solvents (including bulk solution). After L-Phe's lifetimes were determined in DPPC vesicle solutions, results were compared to L-Phe behavior in the bulk solvents to assign L-Phe's local solvation environment within the lipid bilayer vesicle. The fluorescence properties of L-Phe in each of the bulk solvents are reported in Table 1.

The first observation from Table 1 is the quantum yield of L-Phe is extremely poor in aqueous solvents. The aqueous phase quantum yield of L-Phe is 0.023, much lower than Tyr and Trp where quantum yields are 0.14 and 0.13, respectively.[34-37] The second observation is the quantum yield of L-Phe changes depending on the solvation environment with the largest quantum yield of 0.033

measured in a polar protic solvent, methanol. L-Phe's quantum yield decreases 5-fold to 0.006 in a polar aprotic environment (acetonitrile). A description of how the values reported for each quantum yield in Table 1 were calculated can be found in the Supporting Information. The quantum yield (ϕ_f) and radiative rate (k_f) of L-Phe in aqueous solution and methanol were calculated as a function of temperature with the full list found in the Supporting Information (Table SI-3) with only those values calculated at 20 °C reported in Table 1. The calculated quantum yields of L-Phe in aqueous solution as a function of temperature closely match those reported in literature.[56] The quantum yield and radiative rate of L-Phe in acetonitrile was only calculated at 20 °C due to poor solubility and low absorbance and emission intensities.

Table 1. Fluorescence properties of L-Phe in each of the bulk solvents at 20 °C. The steady-state spectra for L-Phe in each of the bulk solvents can be found in the Supporting Information (Figure SI-9).

solvent	λ_{ex} (nm)	λ_{em} (nm)	τ_f (ns)	φ_f	k_f (10^6 s^{-1})
Aqueous	264	287	6.42	0.023[a]	3.52
Methanol	265	290	6.74	0.033	4.89
Acetonitrile	262	299	3.22	0.006	1.72
Cyclohexane	262	301	1.01 (0.85), 4.51 (0.15)		

[a] Quantum yield were calculated in this study but consistent with literature.[56]

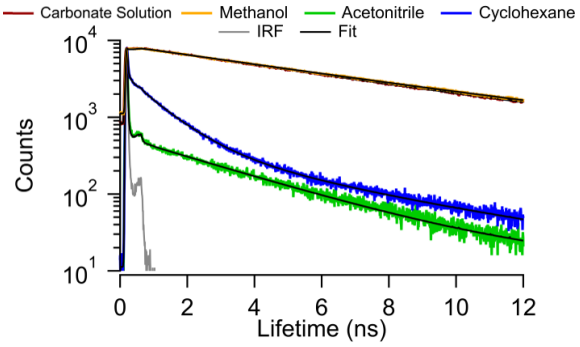

Figure 2. TCSPC spectra of L-Phe in each of the bulk solvents taken at 20 °C. Results from fitting these emission traces to Equation 1 are reported in Table 1. The gray trace is instrument response function (IRF).

The time-resolved fluorescence behaviors of L-Phe in all bulk solvents are shown in Figure 2 with the corresponding fluorescence lifetimes reported in Table 1. L-Phe fluorescence emission in cyclohexane was best fit to two fluorescence decays with the 1.01 ns lifetime as the marker for a nonpolar environment due to the higher amplitude (0.85). The time-resolved fluorescence behaviors of L-Phe in bulk aqueous solution and bulk methanol were measured, separately, as a function of temperature and results are reported Supporting Information (Tables SI-3 and Figure SI-8). The resulting L-Phe lifetimes in carbonate buffer matched those found in literature except for the appearance of a second lifetime at 60 and 70 °C not previously reported.[56] The significance of this second lifetime will be discussed below.

TCSPC in DPPC vesicle solutions

The time-resolved fluorescence behavior of L-Phe in aqueous solution containing DPPC lipid vesicles was characterized as a function of temperature through the $T_{gel\text{-}lc}$ of DPPC (41 °C) up to 70 °C. Time-resolved emission spectra were also acquired as the solution cooled to test for reversibility. The fluorescence decay data are shown in Figure 3 with the corresponding calculated lifetimes and amplitudes reported in Table SI-1. For each temperature, the lifetimes were calculated with the minimum number of lifetimes required for a χ^2 between 0.9 – 1.1. The resulting lifetimes for each temperature were compared to lifetimes found in bulk solvents to correlate local solvation environments experienced by L-Phe within the DPPC lipid bilayer. Each amplitude was radiative rate corrected using the fluorescence quantum yield of L-Phe in aqueous solution and methanol at each corresponding temperature. The explanation for why methanol was chosen to radiative rate correct the amplitude of the second fluorescence lifetime can be found in the Supporting Information.

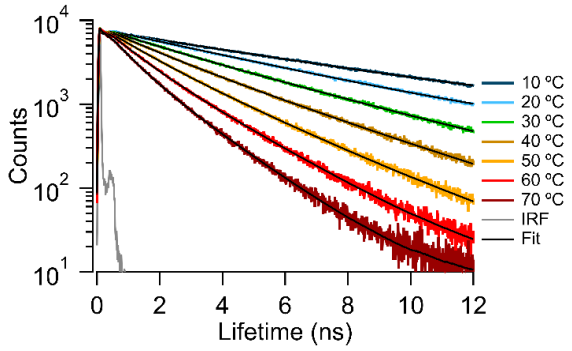

Figure 3. TCSPC spectra of L-Phe in DPPC vesicles as a function of temperature. Results from fitting these emission traces to Equation 1 are reported in Table SI-1.

Fitting the fluorescence decay traces in Figure 3 at both 10 and 20 °C requires only single lifetime (6.6 ns at 10˚C and 4.9 ns at 20˚C). While slightly lower than L-Phe's emission lifetime in the bulk aqueous solution, we assign this emission to L-Phe that remains in the water and not strongly associated with the DPPC vesicles. Once the temperature was raised to 30 °C, however, the decay trace required two lifetimes with the first lifetime corresponding to L-Phe in bulk solution and accounting for 85% of the overall fluorescence decay, and a second lifetime (1.8 ns, 15%) that does not match any result found in bulk solvents but *does* correspond to L-Phe in a polypeptide that is assigned to a different L-Phe rotamer state.[57] This temperature is approximately where the ripple phase (35 °C) occurs for DPPC lipid bilayers. As temperature increases the 2nd lifetime decreases (to 0.7 ns) and the amplitude increases 30%. These results are quantitatively reversible

Given this lifetime's clear correlation with L-Phe in vesicle containing solutions, we assign this lifetime to a new radiative decay pathway for L-Phe associated with the lipid bilayer. While the origin of this new pathway is not immediately apparent, we propose that it results from L-Phe in the bilayer where rotational isomerization is restricted resulting in a shorter fluorescence lifetime

(K_{rot}) that only becomes optically visible when water begins to penetrate into the lipid bilayer. The basis for this assignment is presented in discussion section below.

These data summarized in Figure 4 where changes in the lifetimes and amplitudes are shown as a function of temperature. (The fitting parameters used to generate Figure 4 are reported in Table SI-4 in Supporting Information.) Also shown in Figure 4 is the dashed line corresponding to L-Phe's lifetime in bulk carbonate buffer and two vertical dashed lines that denote DPPC's $T_{gel\text{-}lc}$. Note that the x-axis reporting temperature starts at 10 °C, rises to 70 °C at the axis midpoint and returns to 10 °C. The symmetry shown by all traces about the 70 °C high temperature mark demonstrates reversibility of the observed effects.

Generalizing the effects of L-Phe on vesicle bilayer properties

Given that the 2nd shorter lifetime was attributed to L-Phe associated with the DPPC bilayer that becomes hydrated as the system approaches $T_{gel\text{-}lc}$, additional experiments were carried out to test whether or not this phenomenon was general. These subsequent studies used three other lipid bilayer systems: DSPC (18:0, $T_{gel\text{-}lc}$ = 53.5 °C), DMPC (14:0, $T_{gel\text{-}lc}$ = 22.5 °C), and DLPC (12:0, $T_{gel\text{-}lc}$ = -1.2 °C). All three lipids are phosphatidylcholine (PC) lipids and contain the same headgroup with the only difference being in the length of the saturated acyl chains and corresponding phase transition temperatures.

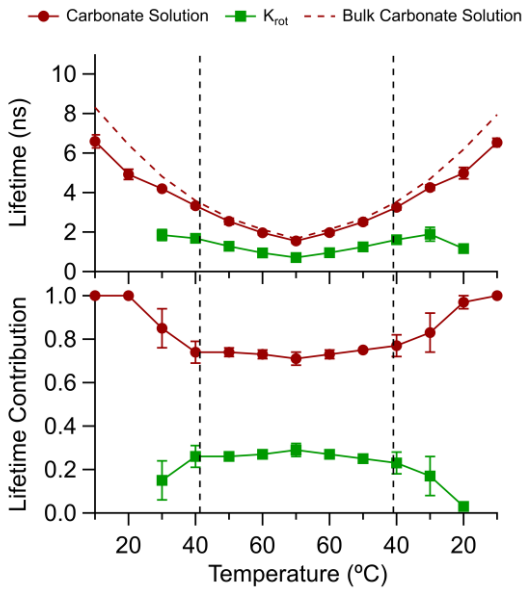

Figure 4. Fluorescence lifetimes (top) and respective radiative rate corrected lifetime contribution (bottom) of L-Phe in DPPC lipid vesicles. The major lifetime is assigned to L-Phe in carbonate buffer (τ_1, burgundy circles), and a restriction of L-Phe rotamer in the DPPC polar headgroup region (τ_2, green squares). The dashed lines indicate the $T_{gel\text{-}lc}$ of the DPPC lipid bilayer at ~41.5 °C. Each point is an average of 3 independent trials and the respective error bars are one standard deviation based on the results of those 3 trials. In some instances, the uncertainty is smaller than the marker used to represent that data point.

The effect L-Phe has on the $T_{gel\text{-}lc}$ was analyzed using DSC with lipid vesicles rehydrated in aqueous solutions (20 mM lipid) as well as with 10 mM L-Phe/vesicle aqueous solutions. Figure 5 shows the DSC traces of DSPC, DMPC, and DLPC in aqueous solution both with and without L-Phe. The same behavior observed in DPPC lipid vesicles is consistent with DSPC and DMPC. Namely, there was no change in the $T_{gel\text{-}lc}$ but there was a decrease in peak intensity. For DSPC and DMPC vesicles, the same peak broadening as in DPPC vesicles was observed. (L-Phe did not affect DLPC's $T_{gel\text{-}lc}$ (at -2˚C) nor did the amplitude of the endotherm change, in stark contrast to DMPC, DPPC and DSPC. DSC data for DLPC with and without L-Phe is shown in Supporting Information, SI-10)

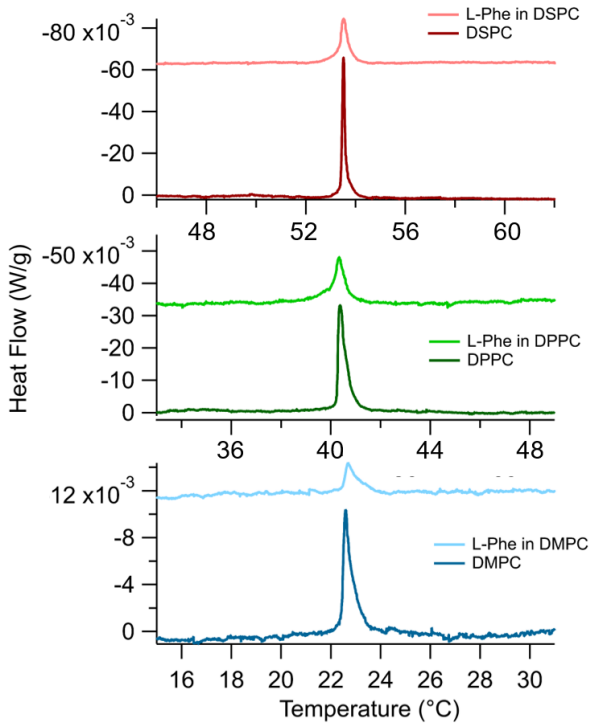

Figure 5. DSC spectra of DSPC (top, red), DPPC (previously shown, middle, green), and DMPC (bottom, blue) vesicle containing solutions rehydrated with carbonate solution and 10 mM L-Phe in carbonate solution. All transitions are endothermic and offset for the ease of viewing.

In a manner similar to studies performed with L-Phe in DPPC vesicle solutions, time-resolved fluorescence behaviors of L-Phe in DSPC, DMPC, and DLPC vesicle solutions were measured as a function of temperature (Figure 6). The temperature regions sampled were adjusted for each lipid vesicle system to capture any behavioral changes with respect to each bilayer's $T_{gel\text{-}lc}$. The data shown in Figure 6 were analyzed in the same way as the L-Phe/DPPC system. (Quantitative fitting parameters are reported in Supporting Information, Table SI-5.

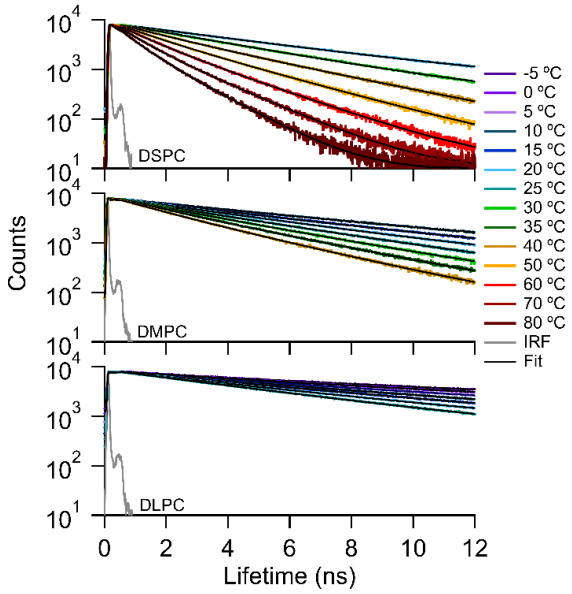

Figure 6. TCSPC spectra of L-Phe in DSPC (top), DMPC (middle), and DLPC (bottom) lipid vesicles as a function of temperature. Results from fitting these emission traces to Equation 1 are reported in Table SI-5.

L-Phe fluorescence emission in all lipid vesicle solutions is described by a single lifetime at low temperatures. For L-Phe in DSPC and DMPC, the appearance of a second lifetime occurs in the vicinity of the respective transition temperatures and, like DPPC, the second lifetime does not match behavior observed in bulk solvents. In DLPC, L-Phe fluorescence is characterized by a single lifetime corresponding to L-Phe fluorescence in bulk solution at all temperatures. From these data, we conclude that L-Phe does not partition into DLPC vesicles. The second general observation is that L-Phe in DSPC and DMPC vesicles behaves similarly to L-Phe in DPPC vesicles. A more detailed assessment is provided below. (Fitting parameters that resulted from analyzing these traces are reported in Supporting Information, Table SI-7.)

Starting with DSPC (18:0, $T_{gel\text{-}lc}$ = 53.5 °C), time-resolved emission was measured every 10 °C between 20 °C to 80 °C. Results in Figure 7 show a major lifetime that corresponds to L-Phe in a bulk solution. For the DSPC vesicle system, the appearance of a second lifetime does not appear

until 40 °C, slightly below the ripple phase of pure DSPC lipid vesicles (~45 °C).[55] The reversibility of L-Phe in DSPC displays the same behavior as seen in DPPC vesicle solutions.

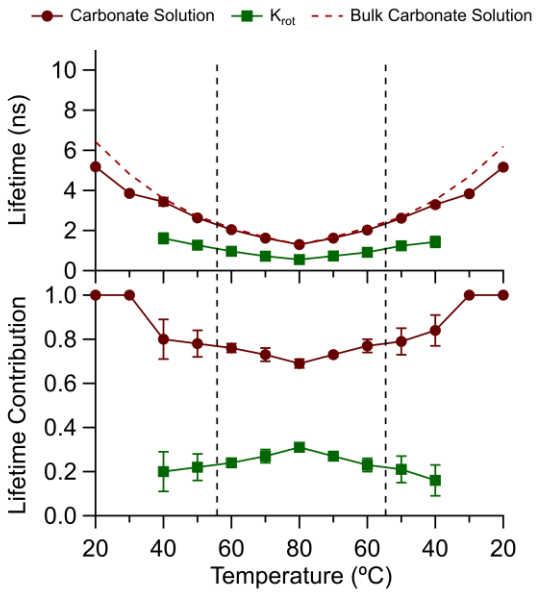

Figure 7. Fluorescence lifetimes (top) and respective radiative rate corrected lifetime contribution (bottom) of L-Phe in a DSPC lipid vesicle solution. The major lifetime is assigned to a L-Phe in carbonate buffer (τ_1, maroon circles), and a second lifetime assigned to L-Phe in the membrane appears at 40˚C (τ_2, dark green squares). The dashed lines indicate the $T_{gel\text{-}lc}$ of the DSPC lipid bilayer at ~53.5 °C. Each point is an average of 3 independent trials and the respective error bars are one standard deviation based on the results of those 3 trials. In some instances, the uncertainty is smaller than the marker used to represent that data point.

Results are not quite so definitive for L-Phe in DMPC vesicle containing solutions. Results in Table SI-5 are shown in Figure 8 and depict the same long lifetime corresponding to L-Phe in in bulk solution. However, the appearance of the second lifetime does not occur until 25 °C or at approximately the same temperature as the DMPC $T_{gel\text{-}lc}$ (22.5°C). This is behavior differs from observations made in DPPC and DSPC lipid vesicle solutions where the second lifetime appeared ~10-12 °C before the $T_{gel\text{-}lc}$.

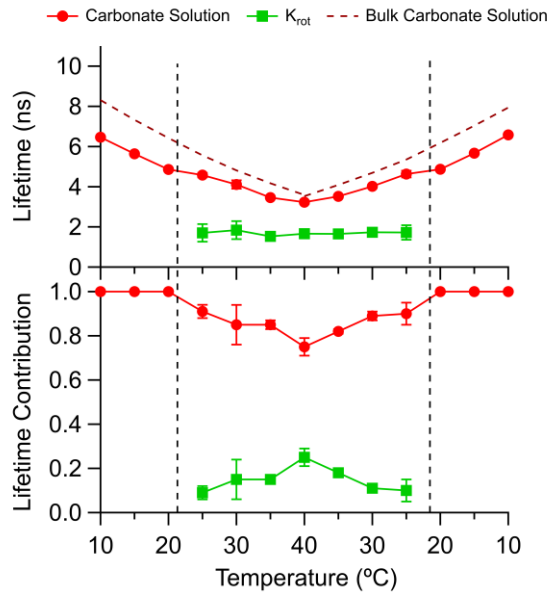

Figure 8. Fluorescence lifetimes (top) and respective radiative rate corrected lifetime contribution (bottom) of L-Phe in a DMPC lipid vesicle solution. The major lifetime is assigned to a L-Phe in carbonate solution (τ_1, red circles), and a second lifetime assigned to L-Phe in the membrane appears at 25 °C (τ_2, light green squares). The dashed lines indicate the $T_{gel\text{-}lc}$ of the DMPC lipid bilayer at 22.5 °C. Each point is an average of 3 independent trials and the respective error bars are one standard deviation based on the results of those 3 trials. In some instances, the uncertainty is smaller than the marker used to represent that data point.

Lastly, DLPC with a pair of C_{12} acyl chains and a $T_{gel\text{-}lc}$ = -1.2 °C shows L-Phe emission with only a single lifetime that is assigned to L-Phe in solution. From these findings, we conclude that L-Phe does not associate in any measurable way with DLPC lipid bilayers. The reasons for this pattern of L-Phe association with lipid bilayers – noticeably with DSPC and DPPC, modestly with DMPC, and not at all with DLPC – are discussed below.

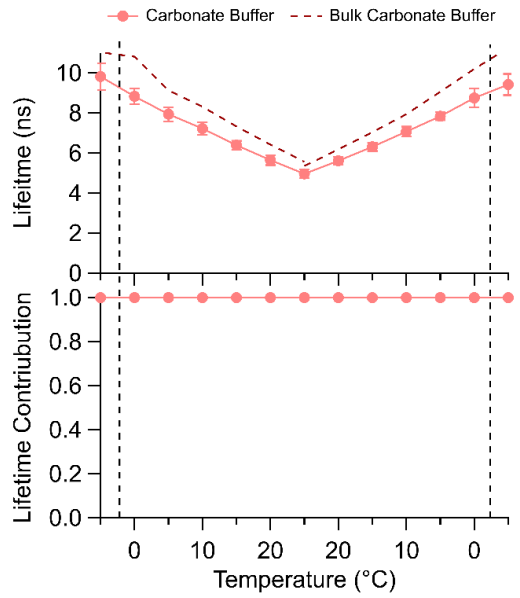

Figure 9. Fluorescence lifetimes (top) and respective radiative rate corrected lifetime contribution (bottom) of L-Phe in a DLPC lipid vesicle solution. The single lifetime is assigned to a L-Phe in carbonate buffer (τ_1, pink circles). The dashed lines indicate the $T_{gel\text{-}lc}$ of the DLPC lipid bilayer at -1.2 °C. Each point is an average of 3 independent trials and the respective error bars are one standard deviation based on the results of those 3 trials. In some instances, the uncertainty is smaller than the marker used to represent that data point.

DISCUSSION:

The partitioning behavior of L-Phe in model biological membranes was characterized using time-resolved fluorescence spectroscopy in combination with differential scanning calorimetry. From results reported above, three discoveries stand out and require discussion:

- DSC data show that L-Phe does not alter bilayer $T_{gel\text{-}lc}$ but does decrease the energy required to melt the bilayer from its gel-phase to its liquid-crystalline phase. This finding applies to DSPC, DPPC and DMPC but *not* to DLPC.

- In the vicinity of $T_{gel\text{-}lc}$, L-Phe time-resolved emission in vesicle solutions begins showing a second, faster emission lifetime (< 2 ns) in addition to the persistent longer lifetime assigned to L-Phe in bulk solution. The shorter L-Phe lifetime is readily apparent in DSPC, DPPC, and DMPC vesicle solutions but *not* in DLPC vesicle solutions. A short lifetime for L-Phe

matching those observed in the vesicle solutions *does* appear in bulk solution at temperatures above 60 °C and this correlation forms the basis of our assignment of this lifetime to a rotamer of L-Phe.

- The 2nd, shorter lifetime in vesicle solutions can comprise up to 30% of the amplitude in the emission decay traces. In DSPC and DPPC vesicle solutions, this shorter lifetime decreases from ~1.8 ns at temperatures just below the $T_{gel\text{-}lc}$ to < 1 ns at 70 °C. Whereas in DMPC vesicles, the lifetime stays almost constant at ~1.6 ns. Furthermore, in DSPC, DPPC and DMPC vesicle solutions the amplitude of the short lifetime contribution rises with temperature.

The discussion below considers each issue individually.

The L-Phe that integrates into the bilayer does not change $T_{gel\text{-}LC}$

The DSC traces in Figures 1 and 5 display the $T_{gel\text{-}lc}$ phase transition behavior for each lipid system studied with and without L-Phe in solution. Two observations stand out. First, L-Phe does not affect the transition temperature for any of the lipid bilayers. The peak in the different endotherms remain at 53.5 °C, 40.4 °C, and 22.5 °C for DSPC, DPPC, and DMPC, respectively, regardless of whether or not L-Phe is present. (The transition temperature for DLPC (-1.2˚C) also remains unchanged as shown in Figure SI-10.) Given that bilayer melting is controlled by van der Waals forces between acyl chains and Coulomb forces between the charged choline headgroups,[46,58] the DSC findings imply that some amount of L-Phe partitions into the gel state bilayer. MacCallum, *et al.* calculated that Phe in the carbonyl and acyl chain region of the bilayer was ~10-12 kJ/mole more stable than in bulk aqueous solution, although these simulations were carried out using a model DOPC bilayer in its fluid, liquid crystalline state.[45] What is clear is that

L-Phe accumulation into the bilayer does not disrupt the fundamental interactions responsible for the transition.

The second observation is that L-Phe *does* change quantitative details related to $T_{gel\text{-}lc}$. For DSPC, DPPC and DMPC, the presence of L-Phe significantly reduces the amount of heat needed to drive the gel-liquid crystalline transition to completion. For vesicle solutions in the absence of L-Phe, the heat required to drive the gel-liquid crystalline transition diminishes with shorter chain length: +60 mW/g for DSPC, +30 mW/g for DPPC and +10 mW/g for DMPC. When L-Phe is added to the solutions, these values drop to 20 mW/g, 14 mW/g, and 3 mW/g for DSPC, DMPC and DLPC respectively. (DLPC shows no change in its $T_{gel\text{-}LC}$ nor in the magnitude of the endotherm and is not considered in this discussion.). This 2-3-fold reduction in the heat required to melt the bilayer in the presence of L-Phe supports the hypothesis that L-Phe partitions into the gel-phase bilayers and disrupts *some* of the chain-chain interactions but this disruption is not extensive enough to completely fluidize the bilayer. In effect, we believe that incorporating L-Phe into the bilayer introduces defects into the long-range order within the frozen chains reducing cooperativity within the bilayer.[59] We note also that the L-Phe's effect on the DSC data scales with L-Phe concentration. As noted at the start of the Results section, we did perform equivalent experiments using solutions of DPPC containing 1, 6, and 8 mM L-Phe, and as L-Phe concentration diminished, the endotherm approached (but never converged) to the endotherm for DPPC vesicles in the absences of L-Phe. These data are shown in Supporting Information, Figure SI-6.

Assigning the 2nd lifetime

To demonstrate the universal behavior of L-Phe in the lipid bilayer vesicle systems, Figure 10 shows all fluorescence lifetimes of L-Phe in DSPC, DPPC, DMPC, DLPC, and bulk carbonate solution across the entire temperature range sampled. Also included on Figure 10 are L-Phe lifetimes in bulk carbonate solution including the second, shorter lifetime that appears only at elevated temperatures (labeled as CS τ_2).

In each vesicle-containing solution, the dominant contribution to the emission decay trace matches L-Phe emission in bulk carbonate solution. This agreement enables us to assign the major lifetime of L-Phe in vesicle-containing solutions to solutes that do not associate with lipid vesicles. In the DSPC, DPPC and DMPC vesicle solutions, the second, shorter lifetime appears at temperatures close to each lipid's respective $T_{gel\text{-}lc}$. As noted in the Results section, the time resolved emission of L-Phe in bulk carbonate solution also has a short lifetime that appears at temperatures ≥ 60 °C. This shorter lifetime does not coincide with emission behavior in any bulk organic solvent, although it does match closely the 1.7 ns lifetime assigned to L-Phe in the EGFRtm peptide as reported by Duneau, *et al.*[57]

Multiple studies have either inferred or predicted that the hydrophobic part of L-Phe should insert into the lipid bilayer membrane through membrane surface defects.[26-29, 31, 32] In its gel phase, the lipid bilayer is rigid and will limit the intramolecular conformational freedom of embedded L-Phe. The benzyl-group of L-Phe is believed to extend into the nonpolar tails and L-Phe's zwitterionic carboxylic acid and amino groups are directed towards the lipid's glycero-backbone and headgroup.[26, 32] Olsztynska *et. al.* reported the appearance of a second, shorter L-Phe emission lifetime (2.6 ns) and proposed that this behavior resulted either from protonation of the carboxylic acid or the formation of aggregates that enabled a faster radiative decay pathway.[60] Supporting this

finding are reports of excimer excitation of 100 mM L-Phe in aqueous solution, as evidenced by an emission peak at 320 nm that disappears with decreasing concentration.[56]

Findings presented in this work do not support the proposal that the short lifetime reflects L-Phe aggregation. First, in all three lipid systems where L-Phe shows membrane affinity, the short lifetime amplitude *increases* with increasing temperature. If the short emission lifetime observed in these systems were due to noncovalently bound aggregates, we would expect aggregation to play *less* of a role at higher temperatures, not more. Second, emission spectra of L-Phe in carbonate solution (Supporting Information Figure SI-9) show no evidence of excimer formation at the concentrations used in these experiments. Third, a 4-fold concentration decrease of L-Phe (2.5 mM) in DPPC vesicles showed no change in partitioning behavior from that of 10 mM L-Phe in DPPC lipid vesicles (Supporting Information Figures SI-2 and SI-3 and Table SI-1). The possibility that aggregation and excimer formation controls L-Phe photophysical behavior at high concentrations as reported by Leroy and Laustrait cannot be discounted,[61] but these effects are unlikely to be present at the 10 mM L-Phe concentrations employed in this work.

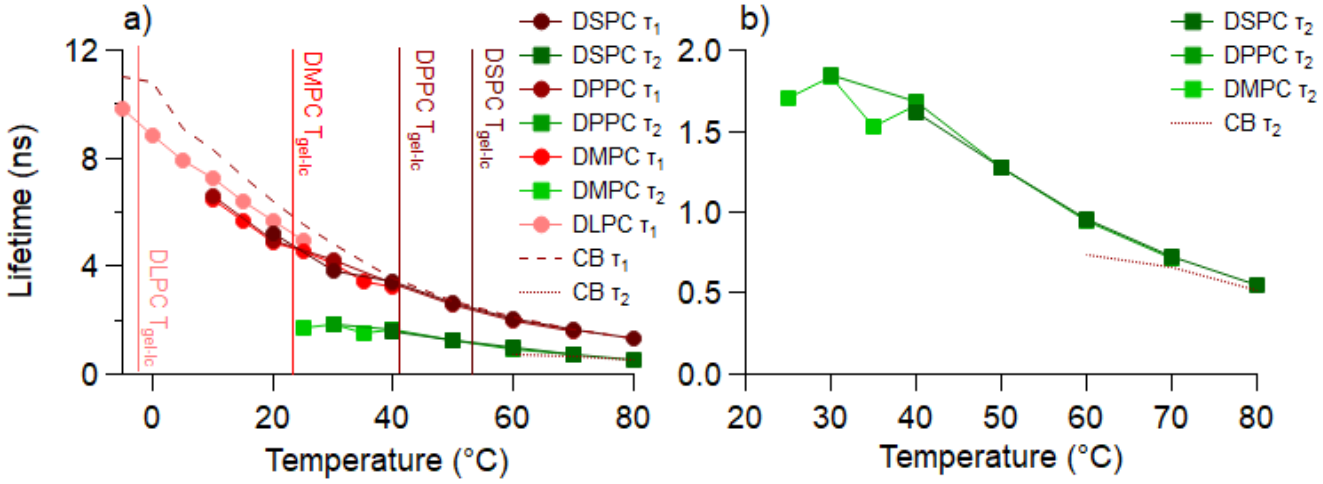

Figure 10. Fluorescence lifetimes of L-Phe in bulk carbonate solution, DSPC, DPPC, DMPC, and DLPC lipid vesicles. Left panel (a) overlays all major lifetimes assigned to a L-Phe in carbonate solution (τ_1: DSPC, maroon circles; DPPC, burgundy circles; DMPC, red

circles, and DLPC, pink circles), and a second lifetime assigned to L-Phe in the membrane appears (τ_2: DSPC, dark green squares; DPPC, green squares; and DMPC, light green squares). Dashed traces indicate L-Phe in bulk carbonate solution (CS) with long dashes indicating first fluorescent lifetime and short dashes indicating second fluorescence lifetime. Solid vertical lines indicate each lipid's $T_{gel\text{-}lc}$ and which are color coded using same scheme as color assignments for lifetime attributed to carbonate solution and labeled as such within figure. Right panel (b) is expanded view of 2nd lifetime alone attributed to restriction of L-Phe rotamer (K_{rot}) in the polar headgroup region of L-Phe in DMPC, DPPC, and DSPC, and bulk carbonate solution (CS). Each point is an average of 3 independent trials of each respective system.

An alternative hypothesis explaining the short L-Phe lifetime was proposed by Duneau, *et al.*, and attributed emission from L-Phe in two different peptides to L-Phe rotamer states at room temperature.[57] In the 29-mer peptide ErbB-2*tm, the single L-Phe residue shows three different emission lifetimes, two of which are sub-ns and a longer, 2.2 ns lifetime. The longer lifetime was assigned to different rotamer states that interconvert on timescales slower than the measured emission lifetimes. L-Phe emission from a second peptide, EGFRtm, is characterized by a single, 1.70 ns lifetime that matches the lifetime observed for L-Phe in the lipid vesicle solutions. The authors proposed that the single lifetime either reflects different rotamers that interconvert rapidly on the timescale of the experiment or L-Phe in a single rotamer state, before concluding that the first explanation, that of rapidly interconverting rotamers, is more consistent with their findings. Similarly, Rzeska *et. al.* analyzed analogues of L-Phe and determined that all possible rotamer conformations result in a similar fluorescence lifetime and are indistinguishable from one another.[43, 44]

In contrast to Duneau, *et. al*, we believe that the short lifetime emission we observe at higher temperatures is due to a single rotamer state. Cavanaugh *et. al.* studied the temperature variations of NMR chemical shifts and coupling of L-Phe rotational isomerization.[62] The authors reported that temperature played a large role in intramolecular and intermolecular parameters of L-Phe, and the importance of these parameters changed depending on the local environment. This NMR study had two conclusions: either the rotamer energies are temperature dependent and gain stability as

temperature increases, or the results require a deviation from the original proposed rotamer structures to understand experimental data.[62] Our findings support the conclusion that a distinctive rotamer structure is stabilized at higher temperatures long enough for a radiative decay pathway to contribute to the overall fluorescence behavior. This stabilization effect of high temperatures is evident in the appearance of a second fluorescence lifetime in bulk carbonate solution starting at 60 °C.

We propose that L-Phe in the bilayer experiences a conformationally restricted environment that forces L-Phe to adopt conformations that decay nonradiatively (as is the case in polar, aprotic environments). As the membrane begins to become more fluid, L-Phe can adopt a rotamer state that *does* decay radiatively. We expect that this emissive state is stabilized by water as water will begin to percolate into the lipid bilayer's polar glycero-backbone region as the system temperature approaches $T_{gel\text{-}lc}$.[63, 64] We believe the second lifetime found in bulk carbonate buffer at 60 °C arises from this same rotamer conformation that is only accessible in bulk solution at higher temperatures, consistent with the first hypothesis proposed by Cavanaugh.[62]

To assess what role the water plays in assisting rotamer formation, the fluorescence lifetimes of L-Phe in a deuterated water (D_2O) carbonate solution were measured as a function of temperature (Supporting Information Table SI-6.) L-Phe in D_2O carbonate solution displays an increase in fluorescence lifetimes (τ_f at 10 °C = 10.81 ns) at low temperatures in comparison to H_2O carbonate solution (τ_f at 10 °C = 8.00 ns). Similarly, the appearance of a second lifetime (0.88 ns, 11%) at 60 °C also occurs in D_2O carbonate solution. However, the amplitude of the second, short lifetime is significantly different as temperature increases from 60 – 80 °C. Namely, the second lifetime displays a sharp increase in amplitude of up to 57% (80 °C) in D_2O carbonate solution in comparison to 20% (80 °C) in H_2O carbonate solution. In D_2O, the hydrogen-bonding capabilities

are stronger than in H_2O. This finding supports our premise that the new emissive rotamer state observed in bilayers close to $T_{gel\text{-}LC}$ and in carbonate solution at elevated temperatures is stabilized by hydrogen bonding and stronger hydrogen bonding (by D_2O) stabilizes this new rotamer even further..

Local solvation environment dependence of the 2nd lifetime of L-Phe in lipid vesicles

The results described above show a strong dependence of L-Phe behavior on bilayer phase with the appearance of the second lifetime. For the DSPC and DPPC lipid vesicles, the appearance of the second lifetime occurs ~10°C before the transition temperature of the lipid bilayer. Uniquely, the second lifetime of L-Phe in DMPC lipid vesicles does not appear until $T > T_{gel\text{-}lc}$. No second lifetime is apparent In DLPC vesicles solutions across the entire temperature range. We propose this second lifetime, assigned to a confined L-Phe rotamer, becomes 'optically visible' only when water is present.

L-Phe in the polar headgroup of the lipid bilayer in its gel phase is subject to a polar, aprotic solvation environment. Our studies of L-Phe in bulk acetonitrile show that in such an environment, fluorescence is weak with the quantum yield of less than 0.01. (In acetonitrile, L-Phe's quantum yield is 0.006 (Table 1).) However, as temperature increases and water percolates into the polar headgroup, hydrogen bonding opportunities become available, and L-Phe can sample a polar, protic solvation environment where its quantum yield is > 5-fold larger (0.033 in methanol) than in polar aprotic environments.

Consequently, we believe that L-Phe in the tightly packed, anhydrous, gel-phase bilayer interior is optically invisible. Bilayer hydration near the gel-liquid crystalline transition temperature allows L-Phe to become optically active and contribute to the overall fluorescence decay. This result

explains why the second lifetime appears at different temperatures for each of the different lipid vesicle systems and in the vicinity of the $T_{gel\text{-}lc}$. For DSPC and DPPC, the second lifetime appears ~10°C before the $T_{gel\text{-}lc}$ and for DMPC, the lifetime appears shortly after the $T_{gel\text{-}lc}$.

Before the lipids fully transition from the gel-phase into the liquid-crystalline phase, they pass through a pre-transition (also known as the ripple phase) where water begins to percolate into the lipid bilayer vesicle.[53, 55] The ripple phase occurs at 16.5 °C, 35 °C, and 46.7 °C for DMPC, DPPC, and DSPC, respectively.[54, 55] Shinoda *et. al.* studied transition temperatures with MD simulations and found the insertion of ethanol into the bilayer creates defects where water can hydrate into the bilayer before the ripple phase and this effect is more pronounced for larger lipids.[65] Therefore, we propose that the L-Phe in the membrane creates a pathway for water to enter the bilayer at or near the ripple phase transition. The onset of the ripple phase and additional membrane hydration is then responsible for the appearance of the second lifetime of L-Phe in DSPC and DPPC vesicles.

As water begins to percolate into the membrane, the bilayer expands by ~25% for DPPC vesicles[66] and transitions into the liquid-crystalline phase of the bilayer where the local solvation environment is polar protic, and solutes have the conformational freedom, the hydrogen bonding and sufficient thermal energy to adopt the new rotamer conformation having the shorter emission lifetime. As seen in Figures 4, 7, and 8, the concentration of L-Phe in the bilayer increases in concentrations up to 30% at high temperatures.

The increase in concentration of the rotamer state implies one of two things: (1) more L-Phe is entering the bilayer as the bilayer expands and experiences this rotamer state. Or (2), as the bilayer expands and water increases concentration within the bilayer, more of the L-Phe that is already in the bilayer becomes optically visible. Scenario (2) seems more likely as the free L-Phe in bulk solvent would not experience a conformational restriction as the vesicles increase and should be

free to adopt a new, thermally accessible rotamer conformation. Instead, the more likely explanation is that L-Phe already in the bilayer becomes optically active (or visible) as the lipid bilayer becomes hydrated.

There is still a remaining question of the second lifetime *after* the $T_{gel\text{-}lc}$ of DMPC lipid vesicles and the absence of a second lifetime in DLPC lipid vesicles. Literature has reported a large temperature dependence of the fluorescence lifetimes of L-Phe in an aqueous solvent.[56] The large temperature dependence is attributed to a switch in the non-radiative decay pathways as a function of temperature. Leroy *et. al.* noted that at temperatures above 0˚C, the main non-radiative decay pathway of L-Phe in aqueous solvents is internal conversion.[56] However, at low temperatures (< 0 °C), the main non-radiative decay pathway begins changing from internal conversion to intersystem crossing.[56] If this switch from internal conversion to intersystem crossing begins to happen at higher temperatures (0-20 °C), then we would not expect to observe a second lifetime in DLPC vesicles and, perhaps, observe a second lifetime in DMPC vesicle solutions above $T_{gel\text{-}lc}$.

CONCLUSION:

Studies reported in this work used time-resolved fluorescence spectroscopy in combination with differential scanning calorimetry to understand the partitioning behavior of L-Phe into model biological membranes. Results show that most L-Phe remains in the carbonate solution, but the L-Phe that *does* partition into the bilayer does not significantly impact the $T_{gel\text{-}lc}$. Evidence of a conformational rotamer fluorescence lifetime of 1.8 ns is seen in DSPC, DPPC, and DMPC lipid vesicles close to their $T_{gel\text{-}LC}$ phase transition temperature. We propose that this rotamer lifetime only becomes optically visible when water penetrates into the bilayer and the local solvation

environment switches from a polar aprotic to a polar protic environment, increasing the quantum yield by an estimated factor of ~5 based on data from L-Phe in methanol and acetonitrile. The L-Phe rotamer lifetime increases slightly in amplitude, eventually comprising up to 30% of the time resolved emission at elevated temperatures. This behavior is predicted to come from L-Phe already in the bilayer that becomes more optically visible as the bilayer expands and increasing amounts of water make the bilayer headgroup region more protic. We hope work reported here sparks further studies into the specifics of the rotamer conformation and related photophysical behaviors of L-Phe, a naturally fluorescent amino acid whose optical properties have been largely overlooked compared to the attention received by other fluorescent amino acids, tyrosine and tryptophan. We also expect that findings reported here will aid in quantifying the behavior of other aromatic amino acids and small peptide chains in lipid vesicle bilayers.

ASSOCIATED CONTENT

Supporting Information. The supporting information contains structures of L-Phe and lipid vesicles used in this work; dynamic light scattering data from vesicle solutions in the presence and absence of L-Phe; steady-state spectra of L-Phe in bulk solvents; fluorescent lifetime, quantum yield, and radiative rate calculations of L-Phe in bulk carbonate buffer and methanol as a function of temperature; and 2.5 mM L-Phe in DPPC lipid vesicles; fluorescence lifetimes of L-Phe in D_2O carbonate buffer as a function of temperature. Also include are the tabulated numerical results from fitting the TCSPC data reported in the manuscript.

AUTHOR INFORMATION

Corresponding Author

Professor Robert A. Walker, Department of Chemistry and Biochemistry and Montana Materials Science Program, Bozeman, MT. 59717. USA

* E-mail: rawalker@montana.edu. Phone: 406-994-7928.

ORCID: 0000-0002-0754-6298

Author Contributions

The manuscript was written through contributions of all authors. All authors have given approval to the final version of the manuscript.

Funding Sources
This material is based upon work supported in part by the National Science Foundation EPSCoR Cooperative Agreement OIA-1757351. Any opinions, findings, and conclusions or recommendations expressed in this material are those of the author(s) and do not necessarily reflect the views of the National Science Foundation.

Notes
The authors declare no competing financial interest.

ACKNOWLEDGMENT

R.C.T. gratefully acknowledges support from the Sloan Indigenous Grant Program

W.H.S. gratefully acknowledges sabbatical support from York College (PA).

C.G. gratefully acknowledges funding from the National Science Foundation Research Experiences for Undergraduates (REU) Program (CHE-1852214).

References.

(1) Jenkins, A.; Andreasen, A.; Trudell, J. R.; Harrison, N. L. Tryptophan scanning mutagenesis in TM4 of the GABA(A) receptor alpha 1 subunit: implications for modulation by inhaled anesthetics and ion channel structure. *Neuropharmacology* **2002**, *43* (4), 669-678. DOI: 10.1016/s0028-3908(02)00175-2.

(2) Patel, A. J.; Honore, E.; Lesage, F.; Fink, M.; Romey, G.; Lazdunski, M. Inhalational anesthetics activate two-pore-domain background K+ channels. *Nature Neuroscience* **1999**, *2* (5), 422-426. DOI: 10.1038/8084.

(3) Choucair, A.; Chakrapani, M.; Chakravarthy, B.; Katsaras, J.; Johnston, L. J. Preferential accumulation of A beta(1-42) on gel phase domains of lipid bilayers: An AFM and fluorescence study. *Biochimica Et Biophysica Acta-Biomembranes* **2007**, *1768* (1), 146-154. DOI: 10.1016/j.bbamem.2006.09.005.

(4) Gaschler, M. M.; Stockwell, B. R. Lipid peroxidation in cell death. *Biochemical and Biophysical Research Communications* **2017**, *482* (3), 419-425. DOI: 10.1016/j.bbrc.2016.10.086.

(5) Rochette, L.; Dogon, G.; Rigal, E.; Zeller, M.; Cottin, Y.; Vergely, C. Lipid Peroxidation and Iron Metabolism: Two Corner Stones in the Homeostasis Control of Ferroptosis. *International Journal of Molecular Sciences* **2023**, *24* (1). DOI: 10.3390/ijms24010449.

(6) Xie, Y.; Hou, W.; Song, X.; Yu, Y.; Huang, J.; Sun, X.; Kang, R.; Tang, D. Ferroptosis: process and function. *Cell Death and Differentiation* **2016**, *23* (3), 369-379. DOI: 10.1038/cdd.2015.158.

(7) Leo, A.; Hansch, C.; Elkins, D. Partition coefficients and their uses. *Chem. Rev.* **1971**, *71* (6), 525-616. DOI: 10.1021/cr60274a001.

(8) Lipinski, C. A. Drug-like properties and the causes of poor solubility and poor permeability. *J Pharmacol Toxicol Methods* **2000**, *44* (1), 235-249. DOI: 10.1016/s1056-8719(00)00107-6.

(9) Lipinski, C. A.; Lombardo, F.; Dominy, B. W.; Feeney, P. J. Experimental and computational approaches to estimate solubility and permeability in drug discovery and development settings. *Adv. Drug Deliv. Rev.* **2001**, *46* (1-3), 3-26. DOI: 10.1016/s0169-409x(00)00129-0.

(10) Ginex, T.; Vazquez, J.; Gilbert, E.; Herrero, E.; Luque, F. J. Lipophilicity in drug design: an overview of lipophilicity descriptors in 3D-QSAR studies. *Future Medicinal Chemistry* **2019**, *11* (10), 1177-1193. DOI: 10.4155/fmc-2018-0435.

(11) Hilal, S. H.; Karickhoff, S. W.; Carreira, L. A. Prediction of the solubility, activity coefficient and liquid/liquid partition coefficient of organic compounds. *Qsar & Combinatorial Science* **2004**, *23* (9), 709-720. DOI: 10.1002/qsar.200430866.

(12) Labute, P. A widely applicable set of descriptors. *Journal of Molecular Graphics & Modelling* **2000**, *18* (4-5), 464-477. DOI: 10.1016/s1093-3263(00)00068-1.

(13) Liang, Y. Z.; Kuo, D. T. F.; Allen, H. E.; Di Toro, D. M. Experimental determination of solvent-water partition coefficients and Abraham parameters for munition constituents. *Chemosphere* **2016**, *161*, 429-437. DOI: 10.1016/j.chemosphere.2016.07.028.

(14) Nicolson, G. L. The Fluid-Mosaic Model of Membrane Structure: still relevant to understanding the structure, function and dynamics of biological membranes after more than 40 years. *Biochim. Biophys. Acta* **2014**, *1838* (6), 1451-1466. DOI: 10.1016/j.bbamem.2013.10.019.

(15) Singer, S. J. N., G.L. The Fluid Mosaid Model of the Structure of Cell Membranes. *Science* **1972**, *175*, 720-731.

(16) Gleason, N. J.; Vostrikov, V. V.; Greathouse, D. V.; Koeppe, R. E. Buried lysine, but not arginine, titrates and alters transmembrane helix tilt. *Proceedings of the National Academy of Sciences of the United States of America* **2013**, *110* (5), 1692-1695. DOI: 10.1073/pnas.1215400110.

(17) Hong, H.; Rinehart, D.; Tamm, L. K. Membrane Depth-Dependent Energetic Contribution of the Tryptophan Side Chain to the Stability of Integral Membrane Proteins. *Biochemistry* **2013**, *52* (25), 4413-4421. DOI: 10.1021/bi400344b.

(18) Vostrikov, V. V.; Hall, B. A.; Sansom, M. S. P.; Koeppe, R. E. Accommodation of a Central Arginine in a Transmembrane Peptide by Changing the Placement of Anchor Residues. *Journal of Physical Chemistry B* **2012**, *116* (43), 12980-12990. DOI: 10.1021/jp308182b.

(19) Piotto, S.; Di Biasi, L.; Sessa, L.; Concilio, S. Transmembrane Peptides as Sensors of the Membrane Physical State. *Frontiers in Physics* **2018**, *6*. DOI: 10.3389/fphy.2018.00048.

(20) Zeno, W. F.; Thatte, A. S.; Wang, L. P.; Snead, W. T.; Lafer, E. M.; Stachowiak, J. C. Molecular Mechanisms of Membrane Curvature Sensing by a Disordered Protein. *Journal of the American Chemical Society* **2019**, *141* (26), 10361-10371. DOI: 10.1021/jacs.9b03927.

(21) Perkins, R.; Vaida, V. Phenylalanine Increases Membrane Permeability. *J. Am. Chem. Soc.* **2017**, *139* (41), 14388-14391. DOI: 10.1021/jacs.7b09219.

(22) Nandi, S.; Pyne, A.; Ghosh, M.; Banerjee, P.; Ghosh, B.; Sarkar, N. Antagonist Effects of l-Phenylalanine and the Enantiomeric Mixture Containing d-Phenylalanine on Phospholipid Vesicle Membrane. *Langmuir* **2020**, *36* (9), 2459-2473. DOI: 10.1021/acs.langmuir.9b03543.

(23) Nandi, S.; Ghosh, B.; Ghosh, M.; Layek, S.; Nandi, P. K.; Sarkar, N. Phenylalanine Interacts with Oleic Acid-Based Vesicle Membrane. Understanding the Molecular Role of Fibril-Vesicle Interaction under the Context of Phenylketonuria. *J. Phys. Chem. B* **2021**, *125* (34), 9776-9793. DOI: 10.1021/acs.jpcb.1c05592.

(24) Griffith, E. C.; Perkins, R. J.; Telesford, D. M.; Adams, E. M.; Cwiklik, L.; Allen, H. C.; Roeselova, M.; Vaida, V. Interaction of L-Phenylalanine with a Phospholipid Monolayer at the Water-Air Interface. *J. Phys. Chem. B* **2015**, *119* (29), 9038-9048. DOI: 10.1021/jp508473w.

(25) Duncan, K. M.; Steel, W. H.; Walker, R. A. Amino acids change solute affinity for lipid bilayers. *Biophys. J.* **2021**, *120* (17), 3676-3687. DOI: 10.1016/j.bpj.2021.07.021.

(26) Cutro, A. C.; Disalvo, E. A. Phenylalanine Blocks Defects Induced in Gel Lipid Membranes by Osmotic Stress. *J. Phys. Chem. B* **2015**, *119* (31), 10060-10065. DOI: 10.1021/acs.jpcb.5b05590.

(27) Chakrabarti, A. C. Permeability of membranes to amino acids and modified amino acids: Mechanisms involved in translocation. *J. Amino Acids* **1994**, *6*, 213-229.

(28) Chakrabarti, A. C.; Deamer, D. W. Permeability of lipid bilayers to amino acids and phosphate. *Biochim. Biophys. Acta* **1992**, *1111*, 171-177.

(29) Cutro, A. C.; Disalvo, E. A.; Frias, M. A. Effects of Phenylalanine on the Liquid-Expanded and Liquid-Condensed States of Phosphatidylcholine Monolayers. *Lipid Insights* **2019**, *12*, 1-9. DOI: 10.1177/1178635318820923.

(30) Johansson, A. C.; Lindahl, E. The role of lipid composition for insertion and stabilization of amino acids in membranes. *J. Chem. Phys.* **2009**, *130* (18), 185101. DOI: 10.1063/1.3129863.

(31) MacCallum, J. L.; Bennett, W. F.; Tieleman, D. P. Distribution of amino acids in a lipid bilayer from computer simulations. *Biophys. J.* **2008**, *94* (9), 3393-3404. DOI: 10.1529/biophysj.107.112805.

(32) Rosa, A. S.; Cutro, A. C.; Frias, M. A.; Disalvo, E. A. Interaction of Phenylalanine with DPPC Model Membranes: More Than a Hydrophobic Interaction. *J. Phys. Chem. B* **2015**, *119* (52), 15844-15847. DOI: 10.1021/acs.jpcb.5b08490.

(33) White, S. H. W., W, C. Hydrophobic interactions of peptides with membarne interfaces. *Biochim. Biophys. Acta* **1998**, *1376*, 339-352.

(34) Bent, D. V. H., E. Excited State Chemistry of Aromatic Amino Acids and Related Peptides. II. Phenylanine. *J. Am. Chem. Soc.* **1974**, *97(10)*, 2606-2612.

(35) Chen, R. F. Fluorescence Quantum Yields of Tryptophan and Tyrosine. *Anal. Lett.* **1967**, *1* (1), 35-42. DOI: 10.1080/00032716708051097.

(36) Mittal, L. J.; Mittal, J. P.; Hayon, E. Primary processes in the photochemistry of phenylalanine and derivatives in aqueous solution. Biphotonic photoionization and photodissociation reactions. *J. Am. Chem. Soc.* **2002**, *95* (19), 6203-6210. DOI: 10.1021/ja00800a009.

(37) Mittal, L. J. M., J.P.; Hayon, E. Biphotonic photodissociation of phenylalanine in aqueous solutions at 20 °C. *Chem. Phys. Lett.* **1973**, *18*, 319-322.

(38) Chin, K. K. T.-S., C.C.; McCallum, J.; Jockusch, S.; Turro, N.J.; Scaiano, J.C.; Foote, C.S.; Garcia-Garibay, M.A. Quantitative Determination of Singlet Oxygen Generate4d by Excited State Aromatic Amino Acids, Proteins, and Immunoglobulins. *J. Am. Chem. Soc.* **2008**, *130*, 6912-6913.

(39) Gally, J. A. E., G.M. The Effect of Temperature on the Fluorescence of Some Aromatic Amino Acids and Proteins. *Biochim. Biophys. Acta* **1962**, *60*, 499-509.

(40) Lorenz, U. J.; Rizzo, T. R. Structural melting of an amino acid dimer upon intersystem crossing. *J. Am. Chem. Soc.* **2014**, *136* (42), 14974-14980. DOI: 10.1021/ja507981p.

(41) Omidyan, R.; Ataelahi, M.; Azimi, G. Excited-state deactivation mechanisms of protonated and neutral phenylalanine: a theoretical study. *RSC Adv.* **2015**, *5* (37), 29032-29039. DOI: 10.1039/c5ra00630a.

(42) Tournon, J. E.-B. A. Intramolecular Charge-Transfer Interactions in Benzyl Derivatives. *J. Chem. Phys.* **2015**, *56*, 5128-5134. DOI: 10.1063/1.4926998.

(43) Rzeska, A.; Stachowiak, K.; Malicka, J.; Lankiewicz, L.; Wiczk, W. Photophysics of phenylalanine analogues - Part 1. Constrained analogues of phenylalanine modified at phenyl ring. *J. Photochem. Photobiol. A. Chem.* **2000**, *133* (1-2), 33-38. DOI: Doi 10.1016/S1010-6030(00)00229-X.

(44) Rzeska, A. M., J.; Stachowiak, K; ; Szymariska, A.; Lankiewicz, L.; Wiczk, W. Photophysics of phenylalanine analogues Part 2. Linear analogues of phenylalanine. *J. Photochem. Photobiol. A. Chem.* **2001**, *140* (1), 21-26. DOI: Doi 10.1016/S1010-6030(01)00394-X.

(45) MacCallum, J. L.; Bennett, W. F. D.; Tieleman, D. P. Distribution of amino acids in a lipid bilayer from computer simulations. *Biophysical Journal* **2008**, *94* (9), 3393-3404. DOI: 10.1529/biophysj.107.112805.

(46) Alanso, A. G., Felix M. Effect of Detergents and Fusogenic Lipids on Phospholipid Phase Transitions. *J. Membr. Biol.* **1983**, *71*, 183-187.

(47) Chapman, D. U., J.; Keough, K.M. Biomembrane Phase Transitions. *J. Biol. Chem.* **1974**, *249*, 2512-2521.

(48) Jain, M. K. W., Nora Min. Effect of Small Molecules on the Dipalmitoyl Lecthin Liposomal Bilayer: III. Phase Transition in Lipid Bilayer. *J. Membrane Biol.* **1977**, *34*, 157-201.

(49) Link, K. A.; Spurzem, G. N.; Tuladhar, A.; Chase, Z.; Wang, Z.; Wang, H.; Walker, R. A. Cooperative Adsorption of Trehalose to DPPC Monolayers at the Water-Air Interface Studied with Vibrational Sum Frequency Generation. *J Phys Chem B* **2019**, *123* (42), 8931-8938. DOI: 10.1021/acs.jpcb.9b07770.

(50) Duncan, K. M.; Casey, A.; Gobrogge, C. A.; Trousdale, R. C.; Piontek, S. M.; Cook, M. J.; Steel, W. H.; Walker, R. A. Coumarin Partitioning in Model Biological Membranes: Limitations of logP as a Predictor. *J. Phys. Chem. B* **2020**, *124* (38), 8299-8308. DOI: 10.1021/acs.jpcb.0c06109.

(51) Gobrogge, C. A.; Blanchard, H. S.; Walker, R. A. Temperature-Dependent Partitioning of Coumarin 152 in Phosphatidylcholine Lipid Bilayers. *J. Phys. Chem. B* **2017**, *121* (16), 4061-4070. DOI: 10.1021/acs.jpcb.6b10893.

(52) Gobrogge, C. A.; Walker, R. A. Quantifying Solute Partitioning in Phosphatidylcholine Membranes. *Analytical Chemistry* **2017**, *89* (22), 12587-12595. DOI: 10.1021/acs.analchem.7b03964.

(53) de Vries, A. H.; Yefimov, S.; Mark, A. E.; Marrink, S. J. Molecular structure of the lecithin ripple phase. *Proc. Natl. Acad. Sci. U.S.A.* **2005**, *102* (15), 5392-5396. DOI: 10.1073/pnas.0408249102.

(54) Chen, W.; Dusa, F.; Witos, J.; Ruokonen, S. K.; Wiedmer, S. K. Determination of the Main Phase Transition Temperature of Phospholipids by Nanoplasmonic Sensing. *Sci. Rep.* **2018**, *8* (1), 14815. DOI: 10.1038/s41598-018-33107-5.

(55) Lentz, B. R.; Freire, E.; Biltonen, R. L. Fluorescence and calorimetric studies of phase transitions in phosphatidylcholine multilayers: kinetics of the pretransition. *Biochem.* **1978**, *17* (21), 4475-4480. DOI: 10.1021/bi00614a018.

(56) Leroy, E. L., H.; Laustrait, G. Fluorescence lifetime and quantum yield of phenylalanine aqueous solutions. Temperature and concentration effects. *J. Photochem. Photobiol.* **1971**, *13*, 411-421.

(57) Duneau, J. P. G., N.; Cremel, G.; Nullans, G.; Hubert, P.; Genest, D.; Vincent, M.; Gallay, J.; Genest, M. Time resolved fluorescence properties of phenylalanine in different environments. Comparison with molecular dynamics simulation. *Biophys. Chem.* **1993**, *73*, 109-119.

(58) Demetzos, C. Differential Scanning Calorimetry (DSC): a tool to study the thermal behavior of lipid bilayers and liposomal stability. *J. Liposome Res.* **2008**, *18* (3), 159-173. DOI: 10.1080/08982100802310261.

(59) Majhi, P. R. B., A. Temperature-Induced Micelle-Vesicle Transitions in DMPC-SDS and DMPC-DTAB Mixtures Studied by Calorimetry and Dynamic Light Scattering. *J. Phys. Chem. B* **2002**, *106*, 10753-10763.

(60) Olsztynska, S. K., M.; Dupuy, N. Influence of Near-Infrared Radiation on the pK_a values of L-Phenylalanine *J. Appl. Spectrosc.* **2006**, *60*, 648-652.

(61) Leroy, E.; Lami, H.; Laustria.G. Fluorescence Lifetime and Quantum Yield of Phenylalanine Aqueous Solutions. Temperature and Concentration Effects. *Photochemistry and Photobiology* **1971**, *13* (5), 411-421. DOI: DOI 10.1111/j.1751-1097.1971.tb06132.x.

(62) Cavanaugh, J. R. The rotational isomerism of phenylalanine by nuclear magnetic resonance. *J. Am. Chem. Soc.* **1967**, *89* (7), 1558-1564. DOI: 10.1021/ja00983a004.

(63) Stephinewski, M. B., A.; Pasenkiewicz-Gierula, M.; Karttunen, M.; Rog, T. Effects of the Lipid Bilayer Phase State on the Water Membrane Interface. *J. Phys. Chem. B* **2010**, *114*, 11784-11792.

(64) Pasenkiewicz-Gierula, M.; Baczynski, K.; Markiewicz, M.; Murzyn, K. Computer modelling studies of the bilayer/water interface. *Biochim. Biophys. Acta* **2016**, *1858* (10), 2305-2321. DOI: 10.1016/j.bbamem.2016.01.024.

(65) Shinoda, W. Permeability across lipid membranes. *Biochem. Biophys. Acta* **2016**, *1858* (10), 2254-2265. DOI: 10.1016/j.bbamem.2016.03.032.

(66) Kucerka, N.; Nieh, M. P.; Katsaras, J. Fluid phase lipid areas and bilayer thicknesses of commonly used phosphatidylcholines as a function of temperature. *Biochim Biophys Acta* **2011**, *1808* (11), 2761-2771. DOI: 10.1016/j.bbamem.2011.07.022.

Table of Contents artwork